REFERÊNCIA

MURILO, A. et al. Fast model predictive control scheme for attitude control systems of rigid-Flexible satellite. In: International Conference on Structural Engineering Dynamics, 2019, Viana do Castelo, Portugal. **Proceedings** [...]. Viana do Castelo, Portugal: Universidade de Lisboa, 2019.

FAST MODEL PREDICTIVE CONTROL SCHEME FOR ATTITUDE CONTROL SYSTEMS OF RIGID-FLEXIBLE SATELLITE

Murilo, A.[1], Peixoto, P. J. D.[1], Souza, L. C. G.[2], Lopes, R. V.[1]

[1]*University of Brasília - Faculty of Gama*
Área Especial de Induústria Projecão A, 72444-240, Brasília, Brazil
[2]*Federal University of ABC*
Av. dos Estados, 09210-580, Santo André, Brazil
andremurilo@unb.br

ABSTRACT
In recent years, the applications related to artificial satellites have considerably grown in several areas such as telecommunications, astronomy and meteorology. An important point that must be taken into account to place a satellite in orbit is the design of Attitude Control System (ACS) to control the angular position according to a fixed reference frame. Most satellites have in their structure the presence of flexible appendices such as solar panels, sails, or even antennas that may produce undesirable oscillations during satellite maneuvers and this can excite the whole system's structure. Therefore, it is important to develop an ACS that limits the excursion of the flexible structure and meet the control requirements for attitude stabilization. In this paper, a Model Predictive Control (MPC) scheme is proposed for ACS of a Rigid-Flexible Satellite. MPC handles structurally the system's constraints in problem formulation by solving at each sampling instant an optimization problem that express the control objectives. As a result, MPC is able to track efficiently the references for attitude control by keeping the displacement of flexible structure within predetermined limits reducing vibration of the system. Moreover, MPC also deals with constraints on control inputs since actuators are physically bounded by its maximum allowable value. Another important feature of the proposed control strategy is the parameterization of MPC which reduces considerably the complexity of the optimization problem enabling short computation times. Simulation results are shown to emphasize the efficiency of the parameterized MPC strategy and a comparison with a Linear Quadratic Regulator (LQR) is also performed.

KEYWORDS: Parameterized MPC, Constraints, Attitude Control System, Rigid-Flexible Satellite

1. INTRODUCTION

There are several methodologies to design satellite Attitude Control System (ACS), depending on the control system complexity; computer simulation cannot be the more appropriate one [1]. Experimental platforms have the important advantage of allowing the satellite dynamics representation in laboratory to accomplish experiments and simulations to evaluate satellites ACS [2]. Experimental test has also the possibility of introducing more realism than the simulation; but it has the difficulty of reproducing zero gravity and torque free space condition. Examples of simulator dynamics and control system experimental investigations can be found in [3, 4]. A classic case of a phenomenon that was not investigated experimentally before launch, was the dissipation energy effect that has altered the satellite Explorer I rotation [5]. Several institutions and universities are investigating and testing the ACS performance by experimental prototypes [6, 7]. In [8, 9] it was showed that the influence of the non-linearities introduced by the slosh motion, the panel's flexibility and the system parameters variation can degrade the control system performance, indicating the necessity of new robust control technique. Examples of multi-objectives control methods to design controller's space system can be found in [10, 11].
Among these techniques, those that use Model Predictive Control (MPC) theory are interesting, since they take into account, in the design, the constraints inherent to the model to be controlled, or to the actuators of the system. Such constraints are easily implemented using predictive control. Several works have been performed in the control area,

using predictive control techniques, potentially in aerospace applications, showing the relevance of this technique for this field of activity. In [12], it is shown that the main purpose of MPC method is to control plants where the implementation of an offline control is very complicated, particularly due to inherent process constraints. Restrictions are present in almost every type of process, such as limiting force on actuators and safety limits for temperatures and speeds. In [13], the MPC technique was used to control the attitude of a micro satellite. The satellite used was the European Space Agency (ESA) and the results were displayed in terms of simulations. An approach using MPC was also proposed by [14] to control the attitude of a satellite. The authors used a hybrid solution for the actuating devices of the system: a combination of reaction wheels and magnetic torque actuators, in case one actuator failed, the other continued to operate, and the process would continue to be properly controlled. Simulations were performed with the proposed control model, which proved good performance of the controller. However, an important drawback of MPC based controller is the computation time to perform on-line optimization which may demand more hardware processing and avoid real-time implementation for embedded applications.

In this paper, a fast MPC scheme is proposed for attitude control of a rigid-flexible satellite that takes into account operational constraints of the system. Moreover, a parameterized approach is also developed in order to diminish the computational burden necessary for on-line optimization. The system modeling considers the same representation used by [8] and [15] and simulation results are shown to verify the advantages of using this method and a comparison with a Linear Quadratic Regulator (LQR) is also provided. This paper is organized as follows. First the rigid-flexible satellite model is presented. Then, the control design of a parameterized MPC strategy is formalized. Some simulation results are shown in the sequel and the paper ends with conclusions and future works.

2. RIGID-FLEXIBLE SATELLITE MODEL

The rigid-flexible satellite model is represented by the rotary flexible link module which consists of a rigid central hub connected to a flexible appendage [16] and the robust performance objectives are associated with the multi-input multi-output model [17, 18], which can be interpreted as a solar panel or a flexible antenna coupled to a rigid satellite. Figure 1 illustrates the satellite system model.

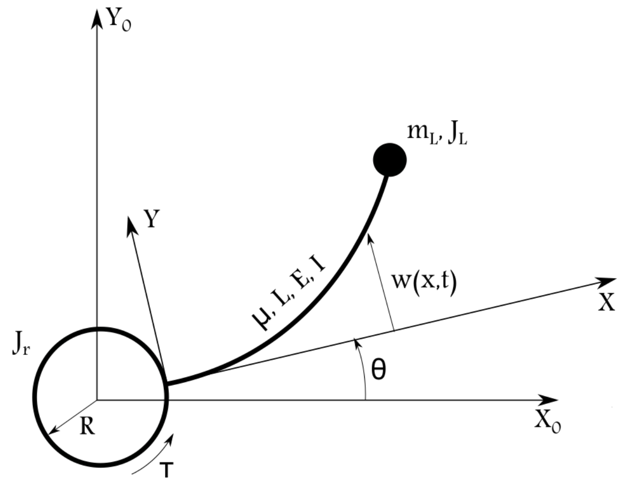

Figure 1 – Rigid-flexible satellite model. Adapted from [15]

In this model, the rigid body of satellite is the rotor with cylindrical geometry of radius R and moment of inertia J_r in relation to the axis of symmetry of the rotor. The flexible rod of length L and linear density μ is fixed to the rotor and has a concentrated mass m_L at the end of free extremity with moment of inertia J_L in relation of rotor's axis. The rod also has a damping coefficient K_e and stiffness EI where E in the Young modulus and I the sectional moment of inertia of the rod.

It is worth mentioning that inertial reference X_0Y_0 is to be considered, instead of non inertial one, namely XY, fixed to satellite's body which rotates together with it. The angle between these two reference axis is $\theta(t)$ which is also called rigid displacement. However, flexible rod deflects with a greater angle than $\theta(t)$. In order to model the displacement of flexible rod, let us define the elastic rod deformation $w(x,t)$, which is the distance between reference XY to the some intermediate point in the rod, which is dependent on the position x along X-axis and current time t. Then, the free rod extremity will deform $w(L,t)$ with total displacement angle defined such as $\alpha(t)$. Rotor is modeled with viscous friction coefficient b_m with torque τ which is the command input.

For mathematical model of rigid-flexible satellite dynamics, the flexible rod is considered as Euler-Bernoulli beam, where elastic deformations can be formalized according to the following partial differential equation such as:

$$EI\frac{\partial^4 w(x,t)}{\partial x^4}+\mu\frac{\partial^2 w(x,t)}{\partial t^2}=0 \tag{1}$$

This equation has some boundary conditions. The extremity of the rod fixed to rigid body has no flexible displacement. In addition, there are no efforts applied at the free extremity of the rod. Then, the boundary conditions are formalized as follows:

$$\begin{aligned} w(0,t) &= 0 \\ \frac{\partial w(0,t)}{\partial x} &= 0 \\ \frac{\partial^2 w(L,t)}{\partial x^2} &= 0 \\ \frac{\partial^3 w(L,t)}{\partial x^3}-\frac{m_L}{EI}\frac{\partial^2 w(L,t)}{\partial t^2} &= 0 \end{aligned} \tag{2}$$

Above equations defined the Boundary Value Problem (BVP). A widely used method in the literature to solve a BVP is the separation of variables where it is assumed that solution is a product between a function of time $T(t)$ and function of space $X(x)$ such as:

$$w(x,t)=X(x)T(t) \tag{3}$$

Replacing this solution in equation (1) and applying the boundary conditions, $X(x)$ can be obtained [15]:

$$X(x)=K\left[cosh(\beta_i x)-cos(\beta_i x)-\left(\frac{cosh(\beta_i L)+cos(\beta_i L)}{senh(\beta_i L)+sen(\beta_i L)}\right)(senh(\beta_i x)-sen(\beta_i x))\right] \tag{4}$$

In this function K is a normalization constant and β_i are the roots of the following equation:

$$1+cosh(\beta L)cos(\beta L)+\frac{m_L}{\mu L}\beta L(senh(\beta L)cos(\beta L)-cosh(\beta L)sen(\beta L))=0 \tag{5}$$

The flexible rod displacement can be therefore obtained by using the assumed-mode method which consists in considering that flexible displacement is the sum of product between a shape function, define by $\varphi(x)$ and a time-dependent function $\eta(t)$ for n vibration modes according to:

$$w(x,t)=\sum_{i=1}^{n}\varphi_i(x)\eta_i(t) \tag{6}$$

where $\eta_i(t)$ are the generalized coordinates which represent how shape functions vary in time. The shape functions must satisfy the following normalization conditions [19]:

$$\mu\int_0^L \varphi_i(x)\varphi_j(x)dx+m_L\varphi_i(L)\varphi_j(L)=0, i\neq j \tag{7}$$

$$\mu\int_0^L \varphi_i^2(x)dx+m_L\varphi_i^2(L)=1 \tag{8}$$

As a result, the shape function φ_i is the solution of Euler-Bernouli equation and constant K can be obtained by normalization conditions (7) and (8) [19]. Thus, the natural frequencies ω_i of each vibration mode can be computed as follows:

$$\omega_i=\beta_i^2\sqrt{\frac{EI}{\mu}} \tag{9}$$

The Lagrange approach is used in order to obtain the satellite dynamical equations by means of kinetic and potential energies of the system, E_k and E_p respectively. The first one can be computed as the sum of kinetic energy of rotor, rod and mass:

$$E_k=E_k(rotor)+E_k(rod)+E_k(mass) \tag{10}$$

Expanding the above expression according to each part of system, E_k can be obtained:

$$\begin{aligned} E_k=\frac{1}{2}\dot{\theta}^2\left(J_r+\mu\left(\int_0^L w^2dx+\frac{1}{3}(R+L)^3-\frac{1}{3}R^3\right)+m_L(w_L^2+(R+L)^2)+J_L\right)+ \\ \frac{1}{2}\dot{\theta}\left(2\mu\int_0^L \dot{w}(R+s(x))dx+2m_L\dot{w}_L+J_L\left(\frac{\partial\dot{w}}{\partial x}\right)+\frac{1}{2}\left(\mu\int_0^L \dot{w}^2dx+m_L\left(\frac{\partial\dot{w}}{\partial x}\right)\right)\right) \end{aligned} \tag{11}$$

where function s represents the distance from the origin of coordinate system XY to a rod mass element. Then, $\varphi_i(x)$ and $\eta_i(t)$ can be expressed by matrix representation such as:

$$\phi = \begin{bmatrix}\varphi_1(x) & \varphi_2(x) & \dots & \varphi_n(x)\end{bmatrix}^T \quad ; \quad \chi = \begin{bmatrix}\eta_1(t) & \eta_2(t) & \dots & \eta_n(t)\end{bmatrix}^T \tag{12}$$

The potential energy of system is given by the following equation:

$$E_p = \frac{1}{2}EI\int_0^L \left(\frac{\partial^2 w}{\partial x^2}\right)^2 dx \tag{13}$$

This system is also subject to a dissipation function of Rayleigh R such as [19]:

$$R = \frac{1}{2}b_m\dot{\theta}^2 + \frac{1}{2}K_e EI\int_0^L \left(\frac{\partial^2 \dot{w}}{\partial x^2}\right)^2 dx \tag{14}$$

Since Lagrange function is defined such as $L = E_k - E_p$, according to Lagrangian method, L must satisfy the following relationship:

$$\frac{d}{dt}\left(\frac{\partial L}{\partial q_i}\right) - \frac{\partial L}{\partial q_i} + \frac{\partial R}{\partial q_i} = \Gamma_i \tag{15}$$

where q_i are the generalized coordinates of Lagrangian method and can be defined as $q = \begin{bmatrix}\theta & \eta_1(t) & \eta_2(t)\dots\eta_n(t)\end{bmatrix}$ and $\Gamma = \begin{bmatrix}\tau & 0 & 0\dots 0\end{bmatrix}$ represents the generalized torque. Replacing $L = E_k - E_p$ in (15) and expanding the resulting expression, the satellite dynamical equations are obtained:

$$\begin{aligned}\ddot{\theta}[I_t + \chi^T C_{rr}\chi] + \ddot{\chi}^T M_{rf} + \dot{\theta}[2\chi^T C_{rr}\dot{\chi} + b_m] &= \tau \\ \ddot{\theta}M_{rf} + M_{ff}\ddot{\chi} - \dot{\theta}^2 C_{rr}\chi + K_{ff}\chi + B_{ff}\dot{\chi} &= 0\end{aligned} \tag{16}$$

where constants are defined such as:

$$\begin{aligned}
I_t &= J_r + \frac{1}{3}\mu((R+L)^3 - R^3) + m_L(R+L)^2 + J_L & B_{ff} &= K_e EI\int_0^L \frac{d^2\phi}{dx^2}\frac{d^2\phi}{dx^2}^T dx \\
C_{rr} &= \mu\int_0^L \phi\phi^T dx + m_L\phi_L\phi_L^T & K_{ff} &= EI\int_0^L \frac{d^2\phi}{dx^2}\frac{d^2\phi}{dx^2}^T dx \\
M_{ff} &= \mu\int_0^L \phi\phi^T dx + m_L\phi_L\phi_L^T + \frac{1}{2}J_L\frac{d\phi_L}{dx}\frac{d\phi_L}{dx}^T & M_{rf} &= \mu\int_0^L \phi(R+x)dx + m_L(R+L)\phi_L + \frac{1}{2}J_L\frac{d\phi_L}{dx}\frac{d\phi_L}{dx}^T
\end{aligned} \tag{17}$$

According to [15], only the first two vibration modes (9) are significant for system dynamics. For this reason, a reduced nonlinear model based on only two vibration modes was adopted and the set of dynamic equations is obtained as follows:

$$\begin{aligned}
\ddot{\theta} &= (\tau + M_{rf}^{(1,1)}K_{ff}^{(1,1)}\eta_1 + M_{rf}^{(2,1)}K_{ff}^{(2,2)}\eta_2 + M_{rf}^{(1,1)}B_{ff}^{(1,1)}\dot{\eta}_1 + M_{rf}^{(2,1)}B_{ff}^{(2,2)}\dot{\eta}_2 - 2\dot{\theta}\dot{\eta}_1\eta_1 \\
&\quad -2\dot{\theta}\dot{\eta}_2\eta_2 - b_m\dot{\theta} - M_{rf}^{(1,1)}\dot{\theta}^2\eta_1 - M_{rf}^{(2,1)}\dot{\theta}^2\eta_2)/(I_t + \eta_1^2 + \eta_2^2 - M_{rf}^{(1,1)^2} - M_{rf}^{(2,1)^2}) \\
\ddot{\eta}_1 &= \dot{\theta}^2\eta_1 - K_{ff}^{(1,1)}\eta_1 - B_{ff}^{(1,1)}\dot{\eta}_1 - M_{rf}^{(1,1)}((\tau + M_{rf}^{(1,1)}K_{ff}^{(1,1)}\eta_1 + M_{rf}^{(2,1)}K_{ff}^{(2,2)}\eta_2 + M_{rf}^{(1,1)}B_{ff}^{(1,1)}\dot{\eta}_1 + M_{rf}^{(2,1)}B_{ff}^{(2,2)}\dot{\eta}_2 \\
&\quad -2\dot{\theta}\dot{\eta}_1\eta_1 - 2\dot{\theta}\dot{\eta}_2\eta_2 - b_m\dot{\theta} - M_{rf}^{(1,1)}\dot{\theta}^2\eta_1 - M_{rf}^{(2,1)}\dot{\theta}^2\eta_2)/(I_t + \eta_1^2 + \eta_2^2 - M_{rf}^{(1,1)^2} - M_{rf}^{(2,1)^2})) \\
\ddot{\eta}_2 &= \dot{\theta}^2\eta_2 - K_{ff}^{(2,2)}\eta_2 - B_{ff}^{(2,2)}\dot{\eta}_2 - M_{rf}^{(2,1)}((\tau + M_{rf}^{(1,1)}K_{ff}^{(1,1)}\eta_1 + M_{rf}^{(2,1)}K_{ff}^{(2,2)}\eta_2 + M_{rf}^{(1,1)}B_{ff}^{(1,1)}\dot{\eta}_1 + M_{rf}^{(2,1)}B_{ff}^{(2,2)}\dot{\eta}_2 \\
&\quad -2\dot{\theta}\dot{\eta}_1\eta_1 - 2\dot{\theta}\dot{\eta}_2\eta_2 - b_m\dot{\theta} - M_{rf}^{(1,1)}\dot{\theta}^2\eta_1 - M_{rf}^{(2,1)}\dot{\theta}^2\eta_2)/(I_t + \eta_1^2 + \eta_2^2 - M_{rf}^{(1,1)^2} - M_{rf}^{(2,1)^2}))
\end{aligned} \tag{18}$$

where notation $A^{(i,j)}$ is used for the i^{th} line and j^{th} column of matrix A. The above system defines a state vector $x \in \mathbb{R}^n$ with $n = 6$ such as $x = [\theta \quad \eta_1 \quad \eta_2 \quad \dot{\theta} \quad \dot{\eta}_1 \quad \dot{\eta}_2]^T$ and control input $u \in \mathbb{R}^{n_u}$ with $n_u = 1$ and $u = \tau$. Note that system (18) is highly coupled with several nonlinear terms and it will be used to simulate plant model to obtain a more realist behavior of satellite in simulation. However, for control design, it is necessary to perform a linearization procedure around some operating point to obtain a Linear Time Invariant (LTI) system of a classical form $\dot{x}(t) = Ax(t) + Bu(t)$, where $A \in \mathbb{R}^{n\times n}$ and $B \in \mathbb{R}^{n\times n_u}$ are the state and input matrices respectively. Linearizing the system (18) by Taylor method around operating point $\begin{bmatrix}\theta & \chi\end{bmatrix} = \begin{bmatrix}0 & 0 & 0 & \dots & 0\end{bmatrix}$, A and B can be obtained:

$$A = \begin{bmatrix}\frac{\partial f_1}{\partial x_1} & \frac{\partial f_1}{\partial x_2} & \cdots & \frac{\partial f_1}{\partial x_n} \\ \frac{\partial f_2}{\partial x_1} & \frac{\partial f_2}{\partial x_2} & \cdots & \frac{\partial f_2}{\partial x_n} \\ \vdots & \vdots & \ddots & \vdots \\ \frac{\partial f_n}{\partial x_1} & \frac{\partial f_n}{\partial x_2} & \cdots & \frac{\partial f_n}{\partial x_n}\end{bmatrix} \quad ; \quad B = \begin{bmatrix}\frac{\partial f_1}{\partial u_1} & \frac{\partial f_1}{\partial u_2} & \cdots & \frac{\partial f_1}{\partial u_n} \\ \frac{\partial f_2}{\partial u_1} & \frac{\partial f_2}{\partial u_2} & \cdots & \frac{\partial f_2}{\partial u_n} \\ \vdots & \vdots & \ddots & \vdots \\ \frac{\partial f_n}{\partial u_1} & \frac{\partial f_n}{\partial u_2} & \cdots & \frac{\partial f_n}{\partial u_n}\end{bmatrix} \tag{19}$$

Thus, the resulting linear system for the first two vibration modes can be expressed by the following set of equations:

$$\begin{aligned}
\ddot{\theta} &= (\tau + M_{rf}^{(1,1)}K_{ff}^{(1,1)}\eta_1 + M_{rf}^{(2,1)}K_{ff}^{(2,2)}\eta_2 + M_{rf}^{(1,1)}B_{ff}^{(1,1)}\dot{\eta}_1 + M_{rf}^{(2,1)}B_{ff}^{(2,2)}\dot{\eta}_2 - b_m\dot{\theta})/(I_t - M_{rf}^{(1,1)^2} - M_{rf}^{(2,1)^2}) \\
\ddot{\eta}_1 &= -K_{ff}^{(1,1)}\eta_1 - B_{ff}^{(1,1)}\dot{\eta}_1 - M_{rf}^{(1,1)}((\tau + M_{rf}^{(1,1)}K_{ff}^{(1,1)}\eta_1 + M_{rf}^{(2,1)}K_{ff}(2,2)\eta_2 \\
&\quad + M_{rf}^{(1,1)}B_{ff}^{(1,1)}\dot{\eta}_1 + M_{rf}^{(2,1)}B_{ff}^{(2,2)}\dot{\eta}_2 - b_m\dot{\theta})/(I_t - M_{rf}^{(1,1)^2} - M_{rf}^{(2,1)^2})) \\
\ddot{\eta}_2 &= \dot{\theta}^2\eta_2 - K_{ff}^{(2,2)}\eta_2 - B_{ff}^{(2,2)}\dot{\eta}_2 - M_{rf}^{(2,1)}((\tau + M_{rf}^{(1,1)}K_{ff}^{(1,1)}\eta_1 + M_{rf}^{(2,1)}K_{ff}^{(2,2)}\eta_2 \\
&\quad + M_{rf}^{(1,1)}B_{ff}^{(1,1)}\dot{\eta}_1 + M_{rf}^{(2,1)}B_{ff}^{(2,2)}\dot{\eta}_2 - b_m\dot{\theta})/(I_t - M_{rf}^{(1,1)^2} - M_{rf}^{(2,1)^2}))
\end{aligned} \tag{20}$$

The system (20) will be used therefore for MPC design as shown in next topic. First it is necessary to define the control problem to be solved. The aim of satellite attitude control is to track the rigid deflection $\theta(t)$, now called regulated output y_r such as $y_r = \theta(t)$, to a desired regulated output namely y_r^d. Moreover, the flexible displacement at rod's extremity $w(L,t)$ must not exceed some predetermined limits such as:

$$y_c^{min} \leq w(L,t) \leq y_c^{max} \tag{21}$$

where y_c^{min} and y_c^{min} are the minimum and maximum allowable values for $w(L,t)$. Since only two vibration modes are considered, flexible deflection can be obtained according to (6):

$$w(L,t) = \varphi_1(L)\eta_1(t) + \varphi_2(L)\eta_2(t) \tag{22}$$

The controller must also respects the limits the control input $u(t)$ which is the torque τ applied to the system. Then, input constraints is formalized as follows:

$$u^{min} \leq u(t) \leq u^{max} \tag{23}$$

Last constraint concerns the input rate of change, which means that the difference between two successive values $\delta_u(t)$ does not exceed the maximum and minimum bounds, namely δ^{max} and δ^{min} such as:

$$\delta^{min} \leq \delta_u(t) \leq \delta^{max} \tag{24}$$

3. MODEL PREDICTIVE CONTROL DESIGN

3.1. Classical MPC Formulation

Once the system model is presented, next step consists in designing a control strategy to provide tracking performance for attitude control and deal with constraints on control inputs and maximum allowable displacement of flexible rod. First, the linear system obtained in previous section must be discretized at each sampling instant k, *i.e*, $x(k+1) = A_d x(k) + B_d u(k)$ where $A_d \in \mathbb{R}^{n\times n}$ and $B_d \in \mathbb{R}^{n\times n_u}$ are state and input discrete matrix respectively. According to formulation proposed by [20], one can define the future values $\tilde{u}$ for control input over a prediction horizon N such as:

$$\tilde{u}(k) = (u(k) \quad u(k+1)\ldots u(k+N-1))^T \in \mathbb{R}^{N.n_u} \tag{25}$$

Then, future states $\tilde{x}(k)$ can be obtained by applying the above control sequence in the discretized system leading to the following expression:

$$\tilde{x}(k) = (x(k+1) \;\; x(k+2)\ldots x(k+N))^T \in \mathbb{R}^{N.n} \tag{26}$$

At instant $k+2$ the state equation becomes $x(k+2) = A_d x(k+1) + B_d u(k+1)$ which is equivalent to $x(k+2) = A_d^2 x(k) + [A_d B_d \quad B_d][u(k) \quad u(k+1)]^T$. Considering the i^{th} instant such as $i \in \{1,...,N\}$, one can define the state at $k+i$ as follows:

$$x(k+i) = \Phi_i x(k) + \Psi_i \tilde{u}(k) \tag{27}$$

where $\Phi_i = A_d^i$ and matrix Ψ_i can be defined according to:

$$\Psi_i := [A_d^{i-1}B_d, ..., A_d B_d, B_d] \begin{pmatrix} \Pi_1^{(n_u,N)} \\ \Pi_2^{(n_u,N)} \\ \vdots \\ \Pi_i^{(n_u,N)} \end{pmatrix} \quad ; \quad \Pi_i^{(n,N)} := (\underbrace{\mathbb{O}_{n\times n}, ..., \mathbb{O}_{n\times n}}_{\text{(i-1) terms}} \; \mathbb{I}_{n\times n} \; \underbrace{\mathbb{O}_{n\times n}, ..., \mathbb{O}_{n\times n}}_{\text{(N-i) terms}}) \tag{28}$$

The matrix $\Pi_i^{(n,N)} \in \mathbb{R}^{n\times(N.n)}$ selects the i^{th} vector of dimension n which is composed by the concatenation of N of such vectors. However only part of the state or a linear combination of $x(k)$ needs to be regulated or tracked. Then, regulated output $y_r \in \mathbb{R}^{n_r}$ can be defined as follows:

$$y_r(k) = C_r x(k) \tag{29}$$

where $C_r \in \mathbb{R}^{n_r\times n}$ is the output matrix and n_r the dimension of regulated states. The rigid displacement $\theta(t)$ is the only regulated output which implies $n_r = 1$. According to [20], in MPC formulations, the cost function can be defined depending on the state at present instant k, the prediction horizon N and the desired regulated output y_r^d such as:

$$J(\tilde{u}|x(k), y_r^d(k), u^d) := \sum_{i=1}^{N} ||y_r(k+i) - y_r^d(k+i)||^2_{Q_y} + \sum_{i=1}^{N} ||\Pi_i^{(n_u,N)}\tilde{u} - u^d||^2_{Q_u} \tag{30}$$

where $Q_y \in \mathbb{R}^{n_r\times n_r}$ is a penalizing matrix for the trajectory tracking error, $Q_u \in \mathbb{R}^{n_u\times n_u}$ to penalize the excursion of command $\tilde{u}$ and u^d the stationary control at steady state condition. The aim of this cost function is to weigh the desired output and control sequence represented by the first and second sum respectively. Then, expanding calculations on (30) based on previous definition, the cost function can be rewritten such as:

$$J(\tilde{u}|x(k), y_r^d(k), u^d) := \frac{1}{2}\tilde{u}^T H \tilde{u} + F(k)^T \tilde{u} \tag{31}$$

where

$$H := 2\sum_{i=1}^{N}[\Psi_i^T C_r^T Q_y C_r \Psi_i + (\Pi_i^{(n_u,N)})^T Q_u (\Pi_i^{(n_u,N)})] \quad ; \quad F(k) := F_1 x(k) + F_2 y_r^d + F_3 u^d$$
$$F_1 := 2\sum_{i=1}^{N}[\Psi_i^T C_r^T Q_y C_r \Phi_i] \quad ; \quad F_2 := -2\sum_{i=1}^{N}[\Psi_i^T C_r^T Q_y \Pi_i^{(n_r,N)}] \quad ; \quad F_3 := 2\sum_{i=1}^{N}[(\Pi_i^{(n_u,N)})^T Q_u]$$

Expression (31) represents a classical Quadratic Problem (QP) where H is the Hessian matrix, which can be computed off-line as well as matrices F_1, F_2 and F_3. Only matrix $F(k)$ needs to be updated because the dependency on $x(k)$ and y_r^d which is the desired set-point. Next step consists in defining the problem's constraints to formalize the complete QP to be solved in MPC formulation.

The set of constrained outputs, represented by flexible displacement, was previously defined in (21) and can be formalized according to $y_c := C_c x$, where C_c represents the constraint output matrix and y_c must satisfy operational constraints on outputs such as $[y_c^{min}, y_c^{max}]$ which are the lower and upper bounds respectively for the outputs. As a result, for $i \in \{1,...,N\}$, expression (21) can be rewritten, *i.e.*, $y_c^{min} \leq y_c(k+i) = C_c x(k+i) \leq y_c^{max}$ and together with (27) a new set of inequalities can be formalized as follows:

$$\begin{pmatrix} +C_c\Psi_1 \\ \vdots \\ +C_c\Psi_N \\ -C_c\Psi_1 \\ \vdots \\ -C_c\Psi_N \end{pmatrix} \tilde{u} \leq \begin{pmatrix} -C_c\Phi_1 \\ \vdots \\ -C_c\Phi_N \\ +C_c\Phi_1 \\ \vdots \\ +C_c\Phi_N \end{pmatrix} x(k) + \begin{pmatrix} +y_c^{max} \\ \vdots \\ +y_c^{max} \\ -y_c^{min} \\ \vdots \\ -y_c^{min} \end{pmatrix} \tag{32}$$

A compact form of above inequality is proposed

$$A_1 \tilde{u} \leq G_1 x(k) + G_3 \tag{33}$$

where A_1, G_1 and G_3 are the inequality matrices related to output constraints. The second set of constraints (23) refers to control inputs and defines physical restrictions on actuator which is represented by the torque. Therefore, $\forall i \in \{1,...,N\}$, the sequence of future control actions over prediction horizon must respect the following set of input constraints:

$$u^{min} \leq u(k+i-1) \leq u^{max} \tag{34}$$

The last set of constraints consists in defining the limits for input variation, *i.e.*, δ^{max} and δ^{min} that represents maximum and minimum allowable values between two successive control values. This means that $\delta_u^i = u(k+i) - u(k+i-1)$ must satisfy the bounds on input derivatives according to $\delta^{min} \leq \delta_u^i \leq \delta^{max}$, $\forall i \in \{1,...,N\}$. Expanding this expression over the prediction horizon, the resulting matrix inequality is represented as follows:

$$
\begin{pmatrix} +\mathbb{I} & \mathbb{O} & \cdots & \mathbb{O} \\ -\mathbb{I} & +\mathbb{I} & \cdots & \mathbb{O} \\ \vdots & \vdots & \vdots & \vdots \\ \mathbb{O} & \mathbb{O} & \cdots & +\mathbb{I} \\ -\mathbb{I} & \mathbb{O} & \cdots & \mathbb{O} \\ +\mathbb{I} & -\mathbb{I} & \cdots & \mathbb{O} \\ \vdots & \vdots & \vdots & \vdots \\ \mathbb{O} & \mathbb{O} & \cdots & -\mathbb{I} \end{pmatrix} \tilde{u} \leq \begin{pmatrix} +\mathbb{I} \\ \mathbb{O} \\ \vdots \\ \mathbb{O} \\ -\mathbb{I} \\ \mathbb{O} \\ \vdots \\ \mathbb{O} \end{pmatrix} u(k-1) + \begin{pmatrix} +\delta_1^{max} \\ +\delta_1^{max} \\ \vdots \\ +\delta_1^{max} \\ -\delta_1^{min} \\ -\delta_1^{min} \\ \vdots \\ -\delta_1^{min} \end{pmatrix}
$$

A compact matrix representation is then proposed:

$$
A_2\tilde{u} \leq G_2 u(k-1) + G_4 \tag{35}
$$

where A_2, G_2 and G_4 are the matrices related to input variation constraints.

Once the constraints and QP are defined, the constrained optimization problem for general MPC strategy can be formalized. The aim is to find an optimized sequence for control input while handling state and input constraints. Thus, the optimization problem to be solved is formalized:

$$
\begin{gathered} \tilde{u}^{opt}(k) := \arg\min_{u} \left[\frac{1}{2}\tilde{u}^T H \tilde{u} + F^T(k)\tilde{u} \right] \text{ subject to:} \\ A^* \tilde{u} \leq B^*(k) \ \ , \ \ \tilde{u}^{min} \leq \tilde{u} \leq \tilde{u}^{max} \end{gathered} \tag{36}
$$

In the above representation, matrices A^* and $B^*(k)$ are defined such as:

$$
A^* = \begin{pmatrix} A_1 \\ A_2 \end{pmatrix} \quad ; \quad B^*(k) = G_5 x(k) + G_6 u(k-1) + G_7 \tag{37}
$$

where G_5, G_6 and G_7 the following matrices:

$$
G_5 = \begin{pmatrix} G_1 \\ \mathbb{O}_{(2.N.n_u)\times n} \end{pmatrix} \quad G_6 = \begin{pmatrix} \mathbb{O}_{(2.N.n_c)\times n_u} \\ G_2 \end{pmatrix} \quad G_7 = \begin{pmatrix} G_3 \\ G_4 \end{pmatrix}
$$

The solution of optimization problem (36) provides the optimal control sequence $\tilde{u}^{opt}$ and only the first term is applied to the system, according to classical MPC definition [12].

$$
K_{MPC}(x(k)) = \Pi_1^{(n_u,N)}.\tilde{u}^{opt}(k) \tag{38}
$$

where K_{MPC} is the optimal control law and $\Pi_1^{(n_u,N)}$ selects the first part of optimal sequence $\tilde{u}^{opt}$ which is scheduled to be applied at each sampling instant.

3.2. Exponential Parameterization

The control parameterization method aims to reduce the complexity of the optimization problem since the number of degrees of freedom of classical MPC problems may increase unnecessarily. Among many possibilities for control parameterization, the exponential strategy proposed by [20] is a potential candidate due to its simplicity to apply while keeping equivalent performance compared to the original problem but with smaller computation times.

The basic idea of the proposed parameterized scheme consists in providing a suitable change of input variables in order to reduce the number of commands to solve the QP. As a result, an exponential parameterization such as presented in [20] can be defined according to:

$$
u_j(k+i) := \sum_{l=1}^{n_e^{(j)}} \left[e^{\frac{-\lambda_j(i\tau_s)}{(l-1)\alpha+1}} \right] \cdot p_l^{(j)}; \alpha > 1 \tag{39}
$$

where p represents the new set of decision variables, the tuning parameters are represented by λ_j and α, $n_e^{(j)}$ the number of exponential terms, j index the j-th actuator and τ_s the sample time. Note that u is now defined as a linear combination of sum of exponential terms which can be computed off-line. Thus, let us introduce component $m_{j,l}(i)$ as follows:

$$
m_{j,l}(i) := \sum_{l=1}^{n_e^{(j)}} \left[e^{\frac{-\lambda_j(i\tau_s)}{(l-1)\alpha+1}} \right] \tag{40}
$$

As a result, u_j is re-written in a compact way:

$$u_j(k+i) := [M_j(i)] \cdot p^{(j)} \quad ; \quad p^{(j)} \in \mathbb{R}^{n_e^{(j)}} \tag{41}$$

where $M_j(i) \in \mathbb{R}^{1 \times n_e^{(j)}}$ is a vector which gathers all m_j components and can also be computed off-line:

$$M_j(i) := (m_{j,1}(i) \cdots m_{j,n_e^{(j)}}(i)) \tag{42}$$

where p is defined as a new set of decision variables:

$$p := \begin{pmatrix} p^{(1)} \in \mathbb{R}^{n_e^{(1)}} \\ \vdots \\ p^{(n_u)} \in \mathbb{R}^{n_e^{(n_u)}} \end{pmatrix} \tag{43}$$

The matrix transformation expressed by (41) together with (43) defines, for each actuator $j = \{1,...,n_u\}$, the following relationship:

$$u(k+i) = M(i) \begin{pmatrix} p^{(1)} \\ \vdots \\ p^{(n_u)} \end{pmatrix} \quad ; \text{with} \quad M(i) = BlockDiag\left(M_j(i)_{j=1}^{n_u}\right)$$

Considering the above expression over the prediction horizon, *i.e.*, for $i = \{0,...,N-1\}$, $\tilde{u}$ can be finally expressed by the following exponential parameterization:

$$\tilde{u} = \Pi_e \cdot p \quad ; \text{with} \quad \Pi_e := \begin{pmatrix} M(0) \\ \vdots \\ M(N-1) \end{pmatrix} \tag{44}$$

Thus, the optimization problem depending on the new set of decision variable p must be reformulated. Equations (44) and (36) lead to a new cost function:

$$J(p) = \frac{1}{2} p^T \left(\Pi_e^T H \Pi_e\right) p + \left(\Pi_e^T F\right)^T p \tag{45}$$

As a result, the new QP to be solved for the exponential parameterization is defined as follows:

$$\begin{aligned} \tilde{p}_{opt}(k) &:= \arg\min_p [J(p)] \text{ subject to:} \\ A_{red} p &\leq B_{red}(k) \ , \ \tilde{u}^{min} \leq \Pi_e.p \leq \tilde{u}^{max} \end{aligned} \tag{46}$$

where $\tilde{p}_{opt}$ is the solution of the new QP, A_{red} and $B_{red}(k)$ the reduced matrices defined as:

$$A_{red} = \begin{pmatrix} A^*.\Pi_e \\ -\Pi_e \\ +\Pi_e \end{pmatrix} \quad B_{red}(k) = \begin{pmatrix} B^*(k) \\ -\tilde{u}^{min} \\ +\tilde{u}^{max} \end{pmatrix}$$

In the above expression Π_e is computed previously. The resulting computational burden is substantially smaller than standard formulation thanks to the low dimensional decision variable obtained by means of exponential parameterization. In fact, the reduction of computation time is a key issue for embedded applications specially in systems where hardware limitations are imposed or necessary.

4. SIMULATION RESULTS

In this section, some simulation results are presented to evaluate the performance of the parameterized MPC strategy. Simulations were carried out with *Matlab-Simulink* software under an Intel core i5 processor of 1,70 GHz with 4GB RAM. Two scenarios of predictive control were performed, $N = 20$ and $N = 60$, with sampling time τ_s of 20 ms. Constraints on regulated output, namely the flexible deflection $w(x,t)$ was set to $[+5,-5]cm$, torque was limited within the interval of $[-2,+2]Nm$ and bounds of input variation defined at $[-1,+1]N.m/s$. The set-point for rigid deflection $\theta(t)$ was set to 45°. The aim consists in tracking the rigid deflection reference for attitude control while respecting the limits on flexible rod's displacement, torque and rate of change of control variable. It is assumed that the whole state vector x is known. Table 1 summarizes the parameters used for numerical simulations for system plant and MPC controller. Parameters of rigid-flexible satellite were taken according to [15].

Table 1 – Parameters used for numerical simulations

Parameters of Rigid-Flexible Satellite		**MPC Parameters**	
Parameter	Value	Parameter	Value
Length of rod: L	1,5 m	Output constraints: $[y_c^{min}, y_c^{max}]$	[-5,+5] cm
Radius of rotor: R	0,05 m	Input constraints: $[u^{min}, u^{max}]$	[-2,+2] N.m
Viscous friction component: b_m	0,15 m^2/s	Input Variation constraints: $[\delta^{min}, \delta^{max}]$	[-1,+1] N.m/s
Moment of inertia of rotor: J_r	0,3 kg.m^2	Prediction horizon: N	20/60
Linear density of rod: μ	0,54 kg/m	Number of exponentials: n_e	2
Damping coefficient: K_e	0,03	Tuning parameter: α	10
Stiffness of rod: EI	18,4 N.m^2	Tuning parameter: λ	30
Mass of extremity: m_L	0,25 kg	Weighing Matrix: Inputs: Q_u	$\begin{bmatrix}0,1\end{bmatrix}$
Moment of inertia of mass - J_L	0,04 kg.m^2	Weighing Matrix: Regulated Output: Q_y	$\begin{bmatrix}100000\end{bmatrix}$

Moreover, simulations using LQR strategy were also realized in order to compare tracking performance and constraints handling. For each simulation scenario, restrictions on control inputs were imposed and model plant was simulated by means of linear (20) and nonlinear (18) representations. As mentioned previously, nonlinear model considered the two most significant vibration modes that affects the system dynamics. Then, numerical values of system matrices defined in (17) can be obtained:

$$M_{rf} = \begin{pmatrix} 1.1402 \\ 0.0641 \end{pmatrix} \quad ; \quad B_{ff} = \begin{pmatrix} 1.1067 & 0.0001 \\ 0.0001 & 62.0769 \end{pmatrix} \quad ; \quad K_{ff} = \begin{pmatrix} 36.9 & 0 \\ 0 & 2069.2 \end{pmatrix} \quad ; \quad C_{rr} = \mathbb{I}_2 \quad ; \quad M_{ff} = \mathbb{I}_2$$

The first simulation scenario illustrates the system behavior under LQR controller. The weighting matrix for state variables was set to $Q = diag[100 \quad 1 \quad 1 \quad 1 \quad 1 \quad 1]$ and for control input the same as for MPC. Other parameters remained unchanged. Figure 2 shows the rigid and flexible deflection as well as input torque and control variation.

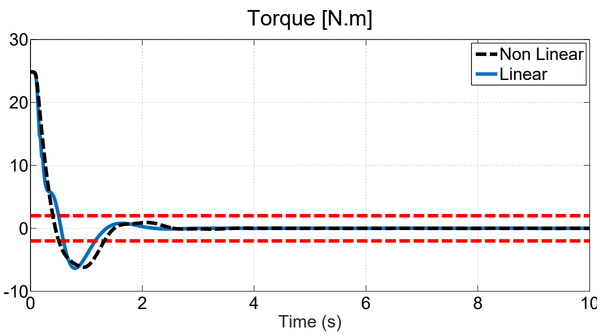

(a) Torque - LQR Controller

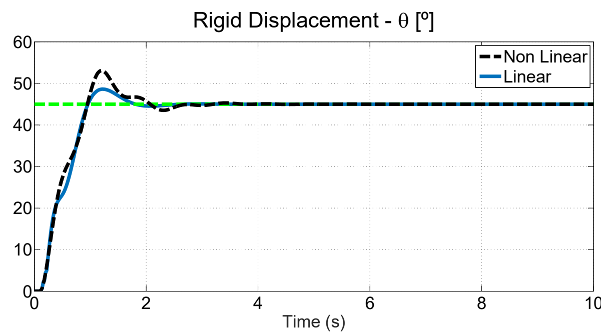

(b) Evolution of Rigid Deflection $\theta(t)$ - LQR

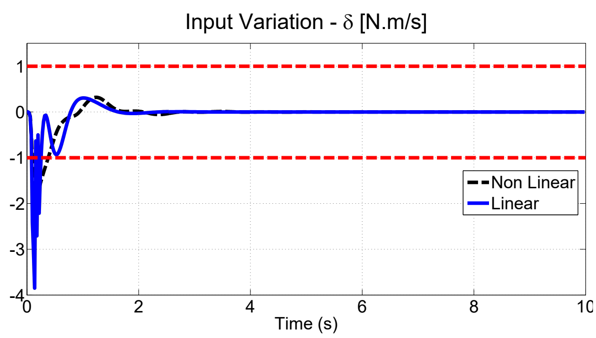

(c) Evolution of Input Rate of Change δ_u - LQR

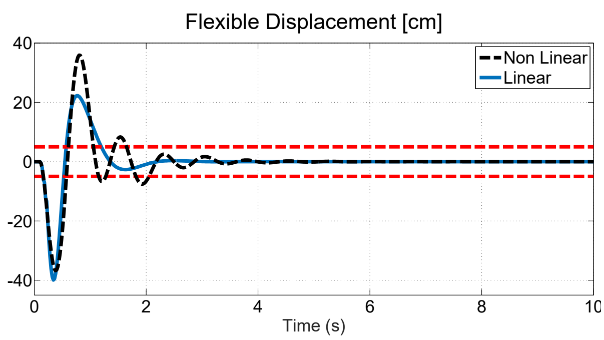

(d) Evolution of Flexible Deflection $w(x,t)$ - LQR

Figure 2 – Simulation scenario of LQR for linear and nonlinear system model. Note that attitude control $\theta(t)$ is tracked with overshoot of 8% (linear) and 18% (nonlinear) but constraints of maximum allowable value for $w(x,t)$, torque input and rate of change are not respected.

The rigid displacement is correctly tracked by LQR with some overshoot observed for both simulation scenarios, linear and nonlinear plant. However, the controller is not able to deal with system's constraints as can be seen in the behavior of flexible deflection, torque and its variation. In fact, LQR is an optimal control strategy for linear systems but with no constraints handling which explains the excursion of transient period of $w(x,t)$, control input u and δ_u.
The second simulation scenario shows the evolution of $\theta(t)$ and $w(x,t)$ using the parameterized MPC method with prediction horizon of 20, as shown in figure 3. It is worth noting that, in this case, the flexible displacement respects the imposed limits for maximal deviation. Moreover, the input torque and control variation also remain within the predetermined interval. For tracking of rigid displacement, the desired reference is attained but with higher overshot and settling time values than LQR. This scenario also shows a closer behavior between linear and nonlinear model.

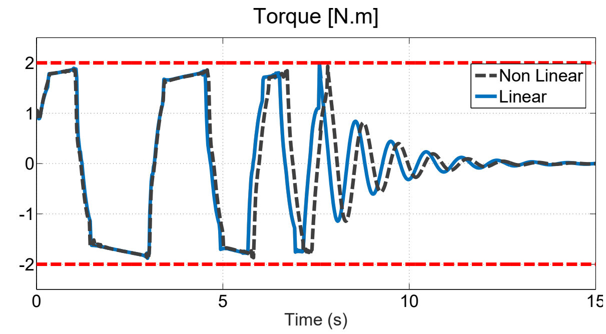

(a) Constrained Torque - MPC Controller ($N = 20$)

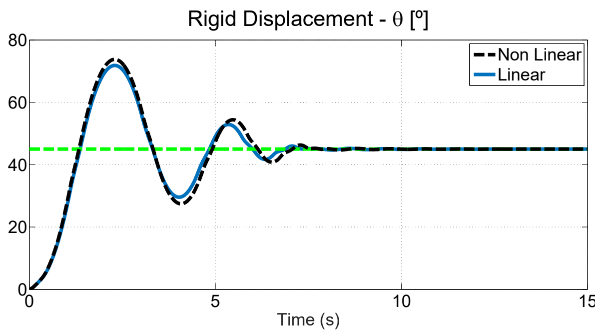

(b) Evolution of Rigid Deflection θ - MPC ($N = 20$)

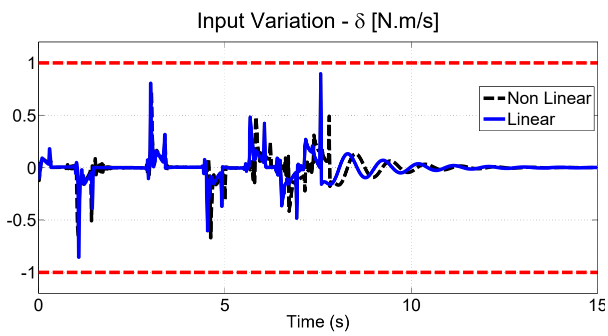

(c) Evolution of Input Rate of Change δ_u - MPC ($N = 20$)

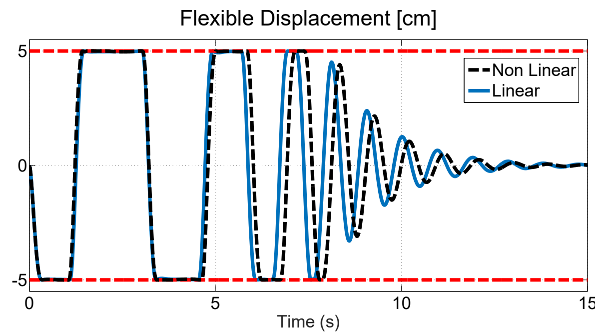

(d) Evolution of Flexible Deflection $w(x,t)$ - MPC ($N = 20$)

Figure 3 – Simulation scenario of MPC for linear and nonlinear system model with $N = 20$. In this case rigid displacement is tracked with an overshoot of 60% and 64% for linear and nonlinear plant respectively, much higher when compared with the previous scenario. On the other hand, output constraints on $w(x,t)$ and control input u and torque variation δ_u are addressed appropriately.

Figure 4 shows the last numerical simulation which proposes the same scenario than previous case but now with higher prediction horizon ($N = 60$). Again, constraints on input and output are structurally respected and almost no difference is observed between response of linear and nonlinear model. Moreover, MPC also deals with constraints on the rate of change of control input, avoiding abrupt variations on actuators which may increase considerably its lifespan. It is worth emphasizing the improvement of transient period of rigid displacement, much better than shorter prediction horizon, enabling smaller overshoot and settling time. In fact, for higher values of prediction horizons, better system performance in terms of stability and optimality are normally expected, specially when model-plant mismatches are not considered [12]. On the other hand, increasing prediction horizon means that a more complex quadratic problem needs to be solved at each sampling instant which also increases the computational burden. This condition is strongly prohibitive when embedded systems are concerned, such as satellite applications, where hardware limitation represents an important issue to be addressed. This motivates the use of more advanced control methodologies, such as parameterized MPC strategy, in order to reduce the complexity of the optimization problem while keeping or improving performance index compared with unconstrained control methods.

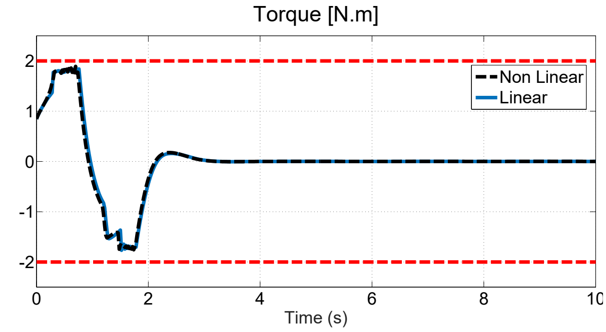

(a) Constrained Torque - MPC Controller ($N = 60$)

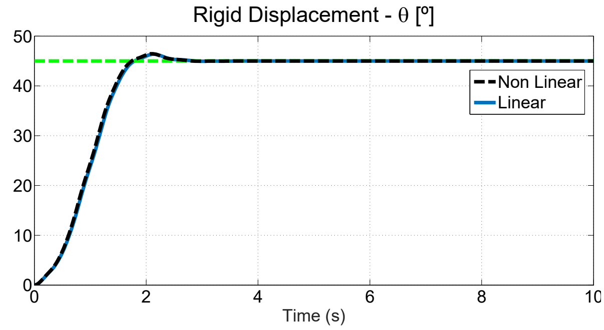

(b) Evolution of Rigid Deflection θ - MPC ($N = 60$)

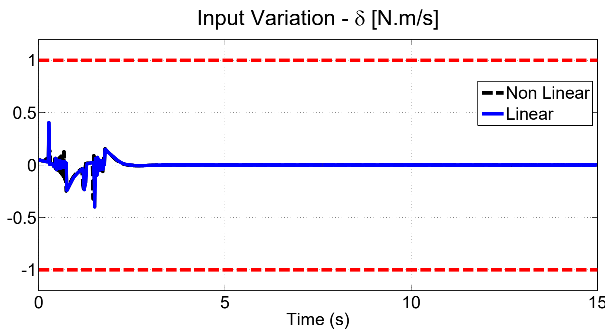

(c) Evolution of Input Rate of Change δ_u - MPC ($N = 60$)

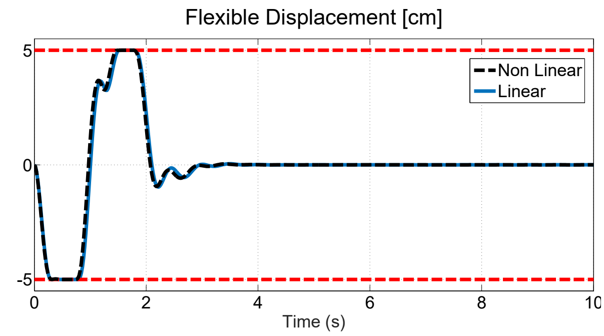

(d) Evolution of Flexible Deflection $w(x,t)$ - MPC ($N = 60$)

Figure 4 – Simulation scenario of MPC for linear and nonlinear system model with $N = 60$. Note an abrupt reduction of overshot for rigid displacement, around 3% for both models, with a settling time of 2.3 seconds, due to the increase of prediction horizon. Flexible deflection also stabilizes faster than the previous case and stays within operational limits. It is worth mentioning the smooth torque's behavior leading to a softer response of $\theta(t)$ and $w(x,t)$.

5. CONCLUSION AND FUTURE WORKS

In this paper, a parameterized MPC technique was proposed for attitude control of a rigid-flexible satellite. Numerical simulations showed the efficiency of this control methodology since satellite operational constraints such as flexible rod displacement and torque were suitably satisfied and tracking performance for attitude angle in terms of overshoot and settling time, represented by the rigid deflection, was attained. Moreover, the exponential parameterization reduced the complexity of the optimization problem enabling the proposed solution to be applied to embedded applications. Future works consist in developing a Hardware-in-the-Loop platform in order to validate the proposed control scheme under real hardware conditions. Preliminary results are quite promising and it will be communicated in future publications.

ACKNOWLEDGEMENTS

The authors would like to acknowledge the financial support of Foundation of Support of Research of the Distrito Federal (FAP-DF), University of Brasilia (UnB) and Brazilian National Research Council (CNPq).

REFERENCES

[1] Hall, C., Tsiotras, P., Shen, H., "Tracking rigid body motion using thrusters and momentum wheels", The Journal of the Astronautical Sciences, 50.

[2] Schwartz, J.L., Peck, M.A., Hall, C.D., "Historical Review of Air-Bearing Spacecraft Simulators", Journal of Guidance, Control, and Dynamics, 26(4), 2003, pp. 513–522.

[3] T Conti, G., Souza, L., "Satellite Attitude Control System Simulator", Shock and Vibration, 15, 2008, pp. 395–402.

[4] Souza, L., Gonzales, R., "Application of the State-Dependent Riccati Equation and Kalman Filter Techniques to the Design of a Satellite Control System", Shock and Vibration, 19, 2012, pp. 939–946.

[5] Kaplan, M., "Modern Spacecraft Dynamics & Control", New York, John Wiley and Sons, Inc., 1976. 427 p.

[6] Kim, B., Velenis, E., Kriengsiri, P., Tsiotras, P., "A spacecraft simulator for research and education", Proceedings of AIAA/AAS astrodynamics specialists conference, 2001, p. 897âĂŞ914.

[7] Sales, T., Rade, D., Souza, L., "Passive vibration control of flexible spacecraft using shunted piezoelectric transducers", Aerospace Science and Technology, 29, 2013, pp. 403–412.

[8] Souza, A., C.G. de Souza, L., "Design of Satellite Attitude Control System Considering the Interaction between Fuel Slosh and Flexible Dynamics during the System Parameters Estimation", Applied Mechanics and Materials, 706, 2014, pp. 14–24.

[9] Bigot, P., "Investigation of the State Dependent Riccati Equation (SDRE) Adaptive Control Advantages for Controlling Non-Linear Systems as a Flexible Rotatory Beam", International Journal of System Application, Engineering & Development, 8, 2014, pp. 92–99.

[10] Mainenti-Lopes, I., Souza, L., De Sousa, F., "Design of a Nonlinear Controller for a Rigid-Flexible Satellite Using Multi-Objective Generalized Extremal Optimization with Real Codification", Shock and Vibration, 19, 2012, pp. 947–956.

[11] Pinheiro, E.R., Souza, L., "Design of the Microsatellite Attitude Control System Using the Mixed Method via LMI Optimization", Mathematical Problems in Engineering, 2013.

[12] Mayne, D., Rawlings, J., Rao, C., Scokaert, P., "Constrained model predictive control: Stability and optimality", Automatica, 36(6), 2000, pp. 789 – 814.

[13] ϕ. Hegrenaes, Gravdahl, J.T., Tondel, P., "Spacecraft attitude control using explicit model predictive control", Automatica, 41(12), 2005, pp. 2107 – 2114.

[14] Xing, Y., Low, K., Pham, M., "Distributed Model Predictive Control of satellite attitude using hybrid reaction wheels and magnetic actuators", Proceedings of ISIEA IEEE Symposium on Industrial Electronics and Applications, 2012, pp. 230–235.

[15] Gu, D.W., Petkov, P., Konstantinov, M., Robust control design with MATLAB, 2005.

[16] Quanser, Rotary Flexible Link, www.quanser.com/products/rotary-flexible-link, 2019.

[17] Skogestad, S., Postlethwaite, I., Multivariable Feedback Control: Analysis and Design, vol. 2, 2005.

[18] Zhou, K., Doyle, J., Essentials of robust control, Prentice Hall, 2019.

[19] Souza, A.G., Estudo do uso de metodos de controle robusto em sistemas espaciais rigidos-flexiveis, Ph.D. thesis, Instituto Nacional de Pesquisas Espaciais (INPE), 2017.

[20] Alamir, M., A Pragmatic Story of Model Predictive Control: Self-Contained Algorithms and Case-Studies, CreateSpace Independent Publishing Platform, 2013.